Submitted to JPCL, 4/5/2024

Energy- and Angle-Resolved Scattering of Ne from Dodecane Liquid Surfaces: Theory Validating Experiment

Junhong Li[1], Hua Guo[2], and Jun Li[1*]

[1] School of Chemistry and Chemical Engineering and Chongqing Key Laboratory of Chemical Theory and Mechanism, Chongqing University, Chongqing 401331, China

[2] Department of Chemistry and Chemical Biology, Center for Computational Chemistry, University of New Mexico, Albuquerque, New Mexico 87131, USA

*To whom correspondence should be addressed: jli15@cqu.edu.cn (JL).

Abstract

The recent combination of the flat-jet and molecular beam techniques by the Neumark group enabled accurate measurements of energy- and angle-resolved product distributions in gas-liquid scattering. Motivated by their experimental work, we present here an all-atom molecular dynamics study of Ne scattering from a dodecane liquid surface, with the objective of elucidating the fundamental aspects of gas-liquid dynamics. Using a fine-tuned general Amber force field, the scattering dynamics simulations were performed at experimental incidence energies and angles, which reproduced semi-quantitatively the measured energy and angular distributions. The branching ratio between the impulsive scattering (IS) and thermal desorption (TD) channels offers extensive dynamical insights. Specifically, the IS / TD branching ratio exhibits a clear correlation with the incidence energy and angle. Ne atoms with lower collision energy are more likely to be trapped by the liquid, yielding an increased number of TD trajectories. For a given collision energy, a large incidence angle led to a higher number of IS trajectories. The energy transfer between Ne atoms and liquid dodecane was found to be more sensitive to the deflection angle than to the incidence angle or the reflection angle. With the increase of deflection angle, the fractional energy loss increases, suggesting more kinetic energy is transferred to the liquid.

Keywords: gas-liquid collisions, molecular dynamics, energy transfer

TOC graphic

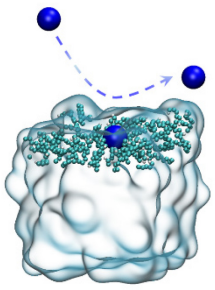

Gas-liquid interfaces are ubiquitous in many natural and man-made environments, including, but not limited to, industrial, atmospheric, biological, and physiological processes.[1-4] These processes are drastically different from those in bulk phases, as the interaction and dynamics between gas-phase molecules and liquid surfaces plays a fundamental role. Hence, understanding these gas-liquid interfacial processes at the microscopic level is of great importance. Unlike the much-studied scattering dynamics in the gas phase or at gas-solid interfaces,[5, 6] it is much more challenging to investigate reactive or nonreactive dynamics at gas-liquid interfaces.[4, 7-9] This is partly due to the fact that a vacuum environment, which is needed to avoid interference of gas-phase collisions, and a clean and well-defined liquid surface are difficult to achieve experimentally. To overcome these hurdles, wetted wheels[10] and micrometer-thin cylindrical jets[11] have been developed to prepare various liquid surfaces. As a result, our understanding of gas-liquid interaction and dynamics has steadily improved, revealing many interesting features. In particular, two limiting cases were found to exist:[8] the impulsive scattering (IS) mechanism for direct bounces of the projectile from the surface without equilibration, and the trapping-desorption (TD) mechanism for stepwise adsorption and thermal desorption mediated by energy dissipation. The two mechanisms possess different final state properties and are thus very useful in characterizing the gas-liquid scattering dynamics.

Despite the ingenious designs, these experimental techniques have their own limitations.[4] The wetted wheel setup is ill-suited for high vapor pressure liquids in a vacuum chamber because of the large surface area, so it is only applicable to liquids with low volatility. Although cylindrical micro-jets are amenable to volatile liquids, they provide only a small scattering target, not ideal for accurate measurement of the scattering angle, one of the most important gas-liquid dynamic observables.[12, 13] Besides, many previous gas-liquid scattering experiments reported incomplete information on the scattering, due to instrumentation design.[14-16] For example, Ne scattering from neat squalane and dodecane liquid surfaces has been investigated using a wetted wheel[14] and/or cylindric microjet[16] with incidence energies (denoted as E_i) at 6 ~ 75 kJ/mol. However, due to instrumental limitations, both the initial (θ_i) and final (θ_f) angles were constrained at 45°, resulting the deflection angle ($\chi = 180° - (\theta_i + \theta_f)$) fixed at 90°.[14-16] In the micro-jet experiment, the absence of a well-defined surface normal leads to large uncertainties in the measured scattering angle.[4]

Very recently, the Neumark group developed a new experimental setup with a microfluidic chip for generating a stable flat liquid jet, and investigated scattering dynamics of Ne (and several small

molecules) from a pure dodecane liquid surface.[12, 13] This new instrument should be more suitable for volatile liquids than the wetted wheel approach[10] and capable of providing a larger and more well-defined scattering target for detecting the scattered atoms and molecules than cylindrical liquid jets.[11] The Neumark group utilized this advanced experimental technique to measure both angle- and energy-resolved dynamic properties for Ne evaporation and Ne scattering from a pure dodecane surface, with unprecedented detail.[12, 13] In particular, "fast" and "slow" Ne with mean incidence energies of 23.7 and 6.3 kJ/mol were directed to the surface at incidence angle (θ_i), defined as the polar angle from the surface normal, of 45°, 60°, or 80°.[12, 13] At the liquid jet temperature 269 K, the exit angle and kinetic energy of the scattered Ne atom were recorded, allowing a detailed analysis of the collision mechanisms and the energy transfer dynamics. In their experiments, the exit angle (θ_f) ranges from 90°−θ_i to 90°, which is much wider than previous experiments. The emergence of such rich dynamic information challenges theory to provide a microscopic characterization of the scattering. To this end, we in this Letter report the first theoretical investigation for Ne scattering from a pure liquid dodecane surface using an all-atom model. As shown below, our dynamic simulations reproduce the experimental measurements quite well, shedding lights on the atomistic details of the dynamics.

Softer and microscopically rougher than solid surfaces, liquid interfaces are disordered, aperiodic, and dynamic with large and constant fluctuation. They possess countless collision sites with different characteristics. To interpret the experimental observations, computational studies are essential. Unlike the extensively investigated gas-phase and gas-solid collisions,[17-19] however, theoretical studies of scattering at liquid surfaces are limited, although the few previous investigations based on classical trajectories have offered considerable insights into the interaction and dynamics.[20-22]

Here, extensive classical molecular dynamics (MD) simulations were carried out to simulate the scattering dynamics. The dodecane surface is modeled as a slab with periodic boundary conditions (PBC), as illustrated in **Figure 1**. The size of the PBC box is 4.5 × 4.5 × 50.0 nm^3, with the liquid slab of ~4.5 nm thickness located 2.0 nm away from the bottom. The upper surface is located near Z = 6.5 nm, but is quite rough. The vacuum space above the surface is thus ~43.5 nm, sufficient for the scattering simulation. The system was first equilibrated at the experimental temperature of 269 K (T_{liq} = 269 K), followed by a 50 ps NVT simulation, from which surface configurations were saved for later scattering simulations. Ne atoms with experimental translational energies of 6.3 (slow) and 23.7

(fast) kJ/mol were directed to the surface from 2.0 nm above the surface. The X and Y coordinates of Ne were uniformly randomized along the X- and Y-axis of the PBC box. The velocity components were set according to the initial kinetic energy and the incidence angle, with the incidence plane parallel to the XZ plane. The scattering dynamics was simulated within an NVE ensemble, with a time step of 1.0 fs. The system contains ~10,000 atoms, the scattering simulations were performed under 6 different initial conditions, for each condition 10,000 trajectories were run to pursue better results with lower statistical error. The trajectory was terminated when the Z coordinate of the Ne atom was higher than its initial value, suggesting the projectile has left the surface. Otherwise, the trajectory was terminated at 500 ps, for which the Ne was considered trapped. To compare with experimental data, we focus on in-plane scattering, which is defined with a range of scattered azimuthal angle of ±10°. According to **Table S5~S11**, the in-plane scattering contributes 7~16% of the entire hemisphere scattering for different initial conditions. **Figure 1** shows the corresponding definition of the in-plane trajectory, and **Figure S1** depicts the coordinates and angles for all trajectories scattered in the hemisphere. Additional details of the simulations can be found in **Supporting Information (SI)**.

Theoretically, the interaction potential must be adequate for describing dodecane both in bulk and at surface. In addition, the interaction between dodecane and Ne also plays a central role in scattering dynamics. In this work, we employ the GAFF (general AMBER force field) all-atom force field,[23] but reoptimized the force-field parameters using first principles data. The form and parameters of the force field, as well as its validation, are given in **SI**. Note that for the current gas-liquid system, the calculation cost based on the classical force field is too huge to be done with only CPU. GPU was finally utilized to accelerate the dynamic simulation. GPU can yield ~1000 ns/day for liquid dodecane, ~700 ns/day for slab, and ~100 ns/day for scattering.

Figure 2 displays four exemplary trajectories observed in the simulations with fast Ne atoms (E_i = 23.7 kJ/mol) at $\theta_i = 45^o$. The same types of trajectories have been observed under other conditions. These trajectories are differentiated by the time evolution of the Z coordinate and kinetic energy of Ne. **Figure 2(a)** presents a typical IS trajectory, which undergoes a single collision near Z~6.5 nm with the Ne atom bouncing directly from the surface within 5 ps. The Ne kinetic energy has only minor changes during the collision process near the smallest Z values and remains slightly lower in the exit channel. The other extreme is depicted by a trapped trajectory in **Figure 2(b)**, which illustrates

the impinging Ne atom diving in the liquid dodecane, evidenced by the Z coordinate below 6 nm. The Ne atom loses its kinetic energy almost completely and is unable to exit the liquid dodecane during the 500 ps simulation time. The fate of the trapped Ne is most likely to desorb with TD characteristics, but our finite simulation length prevented the explicit observation of the final departure. There are only less than 20 such cases in 10,000 trajectories in all simulations (< 0.2%), which represents a negligible minority. The other two panels, **Figure 2(c)** and **2(d)**, the scattering lasted about 30 ps, but they have quite different dynamics. As shown in **Figure 2(c)**, the Ne atom penetrates the liquid surface, as evidenced by frequent changes of its kinetic energy and generally small Z values, and eventually exit after multiple collisions with dodecane molecules. Such a trajectory is characteristic of TD. Alternatively, as shown in **Figure 2(d)**, the Ne atom may traverse the liquid surface near Z = 7 nm and experience multiple IS-like collisions. The duration of each collision is as brief as that of the IS channel, and the kinetic energy does not fluctuate significantly between two collisions after the initial drop. The Z coordinate of Ne atom during such a collision is higher than that shown in **Figure 2 (c)**. Nevertheless, it was found that the contribution for such a long IS mechanism is also quite small (<5%).

The energy transfer between Ne atoms and liquid dodecane is facilitated by the collisions between Ne and surface molecules. A good descriptor of a collision (or kick) is the sign change of the Ne velocity in any of the three components.[22] Not unexpectedly, the number of kicks (N_{kick}) for each trajectory is correlated with the average kinetic energy of the scattered Ne atoms, as shown in **Figure S6**. Hence, we use N_{kick} to identify the IS and TD channels, following similar strategy by Peng et al.[22] As shown in **Figure S6**, for different initial conditions, N_{kick} was chosen so that after which, the Ne kinetic energy is below $2RT_{liq}$, namely, the average energy of the thermally equilibrated atoms effusing from the surface. As summarized in **Table S5**, on average, N_{kick} is 10, identical to the one estimated by Peng et al.[22] Besides, one can see that Ne atoms with smaller incidence energy need fewer N_{kick} to be thermalized than those with larger incidence energy by the liquid under the same incidence angle.

The TD fraction is defined as the number ratio of TD trajectories to the total non-trapped trajectories, namely, the sum of IS and TD trajectories. As displayed in **Figure 3 (a)**, there is a significant portion of TD trajectories at both collision energies. The TD fraction decreases as the incidence angle θ_i increases for a given reflection angle $\theta_f = 60°$. The theory-experiment agreement

is quantitative for 6.3 and 23.7 kJ/mol. The TD fraction as a function of the deflection angle χ was also available from experiment.[13] **Figure 3 (b)** compares our simulated results to the experiment at the incidence angle $\theta_i = 60°$. Clearly, as χ increases, the Ne atoms are scattered closer to the surface normal. The IS trajectories, which show a larger reflection angle θ_f than the incidence angle θ_i, contribute more in the small χ range. In contrast, the TD trajectories, behaving more like evaporation and following the $\cos\theta_f$ angular distribution, contribute to the components in the large χ range. Overall, the different distributions of IS and TD trajectories result in an increase in the TD fraction as the deflection angle χ increases.

Figure 4 (a), **(b)**, and **(c)** compare the calculated and measured in-plane θ_f distributions of scattered Ne atoms at $\theta_i = 45°$, 60°, and 80°, respectively, at $E_i = 23.7$ kJ/mol. **Figure 4 (d), (e), and (f)** display the same results but for $E_i = 6.3$ kJ/mol. One can see that experiment[12, 13] and theory agree reasonably well, although quantitative differences do exist. Evidently, the angular distributions in the TD channel can be reasonably fitted by a cosine function, which suggests that Ne atoms lose memory of their initial states after extensive interaction with liquid dodecane, resembling the distribution of evaporation from the liquid. In contrast, the results for IS significantly differ from those in TD. Most IS trajectories are forward scattered and lie close to the specular angle. For $E_i = 23.7$ kJ/mol and $\theta_i = 45°$, the computed θ_f peak at 60° is in reasonably good agreement with the experimental peak at 50°. At $\theta_i = 60°$, both experiment and theory distributions peak at 70°. For $E_i = 6.3$ kJ/mol, the calculated IS peaks are at $\theta_f = 50°$, 70°, and 70°, respectively, for $\theta_i = 45°$, 60°, and 80°. Namely, Ne in the IS channel tends to scatter nearly specularly, suggesting the approximate conservation the momentum along the surface plane. The corresponding hemispherical distributions with all trajectories considered are depicted in **Figure S7 and S8**, which show that the TD channel is largely isotropic in both the polar and azimuthal angles while the IS channel is dominated by forward near-specular scattering. Such more global distributions have not been reported by experiment.

In Figure 5, velocity distributions of the in-plane scattered Ne are shown for both the IS and TD channels. Following previous work,[12, 13] the TD distributions were fitted in the Maxwell–Boltzmann (MB) flux distribution form:

$$f_{\mathrm{MB}}(v) \propto v^3 \exp\left[-\frac{mv^2}{2RT_{\mathrm{liq}}}\right], \quad (1)$$

where v and m are the final velocity and atomic mass of the Ne atom, and R is the gas constant. The

flux distribution for a supersonic (SS) molecular beam was utilized in fitting the IS distributions:

$$f_{SS}(v) \propto v^3 \exp\left[-\frac{m(v - v_{SS})^2}{2RT_{SS}}\right], \quad (2)$$

where v_{SS} and T_{SS} are the average flow velocity and temperature that need be fitted. The total distribution is the sum of the TD and IS components. Such functions have proven successful in fitting the experimental TOF results,[12] which also validate the theoretical method proposed in this paper to distinguish the two different mechanisms through the number of kicks in the trajectories. The IS trajectories are primarily with high velocities, while the TD trajectories have lower velocities. The overall distribution of translational energy exhibits a single peak, consistent with the experimental TOF spectra.[12, 13]

The fractional energy loss, defined as $\Delta E/E_i$, where $\Delta E = E_i - \langle E_{IS} \rangle$, is commonly used to quantify the kinetic energy transferred from the impinging molecule to the liquid.[7, 24] Here, $\langle E_{IS} \rangle$ denotes the average final translational energy of scattered Ne atoms in the IS channel. Two limiting cases exist: a perfectly elastic collision, where no kinetic energy loss resulting in $\Delta E/E_i = 0$, and a scenario where the Ne atom loses all its energy to the liquid, resulting in a fractional energy loss of 1. **Figure 6** shows that the fractional energy loss depends more on the deflection angle χ than on the incidence angle θ_i or the reflection angle θ_f. At $\theta_i = 60°$, for example, the experimental average fraction energy loss for $\chi = 90°$, 60°, 45°, and 30° were 0.46, 0.32, 0.25, and 0.15. The simulation results are 0.55, 0.41, 0.37, and 0.29, respectively. As the deflection angle increases, the fractional energy loss also increases, indicating more translational energy is transferred to the liquid. This suggests that Ne atoms emitted closer to the liquid surface tend to lose less translational energy, leaning towards elastic collisions. Conversely, Ne atoms emitted in a direction closer to the surface normal tend to lose more translational energy, closer to inelastic collisions. Apparently, our computational results are slightly higher than its experimental counterparts, which show little dependence on θ_i.[13]

As mentioned earlier, many uncertainties associated with previous gas-liquid scattering techniques have been lifted by the recent advent of the flat-jet approach, which enables detailed experiment-theory comparison. Our simulations of Ne scattering from a liquid dodecane surface have achieved semi-quantitative, and quantitative in some cases, reproduction of experimental observations. Such detailed comparisons are important to gain insight into the microscopic details of the scattering dynamics. An important observation in the recent experiments, supported by our

simulations, is the increase of TD fraction with decreasing incidence angle (θ_i),[13] which is in contrast to scattering from a typical solid surface.[25, 26] Similar observations have been made in previous studies, but with more noise.[27-29] The large TD fraction along the surface normal can be largely attributed to more efficient energy loss to the liquid surface. Analysis of the trajectories revealed that Ne atoms with a smaller incidence angle θ_i, having a larger Z component in velocity, penetrate the liquid more easily, thereby increasing the chances for being trapped by the liquid. With decreasing θ_i, the trajectories generally switch from penetrating to grazing. There are of course kinematic factors, but the main differences of a liquid from solid surface are its softness, roughness, and porosity, which help to accommodate the impinging projectile. Although the agreement between experiment and theory is good, deviations do exist. Possible experimental uncertainties include the velocity spread of the incidence Ne beam and product detecting conditions.[13] Theoretically, there might still be errors in the interaction potential between Ne and the dodecane, as discussed in **SI**. It is noted that the machine learning approach has been demonstrated to be very promising in representing the interaction potential of complex condensed phase systems, including the gas-solid interfaces. Similarly, but with more expensive calculation cost, the machine learning approach can be utilized for gas-liquid scattering.

To conclude, our detailed simulations of gas-liquid collision dynamics not only validated the experimental observations, but also gained microscopic insights into atomistic mechanisms. These simulations are complementary to experiments and often necessary to understand the measured results. Furthermore, the advent of advanced hardware and software, especially the utilization of GPUs, has made it feasible to conduct extensive simulations of complex systems that were previously unattainable. Future investigations of molecular scattering from liquid surfaces, reactive or non-reactive, are expected to reveal more detailed dynamics, shedding additional light on the complex interaction between various molecules and liquid surfaces.

Supporting Information

Additional results are given in the Supplementary Information, SI.

Notes

The authors declare no competing financial interests.

Acknowledgments

This work was financially supported by the National Natural Science Foundation of China (Grant No. 21973009), Chongqing Talent Program (Grant No. cstc2021ycjh-bgzxm0070) and the Venture and Innovation Support Program for Chongqing Overseas Returnees (Grant No. cx2021071). HG is grateful to the US National Science Foundation (Grant No. CHE-1951328 and CHE-2306975) for partial support. We also thank Profs. Dan Neumark and Gil Nathanson for useful discussions.

References

(1) Davidovcits, P.; Kolb, C.; Williams, L.; Jayne, J.; Worsnop, D. Mass accommodation and chemical reactions at gas–liquid interfaces. *Chem. Rev.* **2006**, *106*, 1323-1354.

(2) George, I.; Abbatt, J. Heterogeneous oxidation of atmospheric aerosol particles by gas-phase radicals. *Nat. Chem.* **2010**, *2*, 713-722.

(3) Phillips, L. Processes at the gas–liquid interface. *Int. Rev. Phys. Chem.* **2011**, *30*, 301-333.

(4) Faust, J. A.; Nathanson, G. M. Microjets and coated wheels: versatile tools for exploring collisions and reactions at gas-liquid interfaces. *Chem. Soc. Rev.* **2016**, *45*, 3609-3620.

(5) Wang, T.; Yang, T.; Xiao, C.; Sun, Z.; Zhang, D.; Yang, X.; Weichman, M. L.; Neumark, D. M. Dynamical resonances in chemical reactions. *Chem. Soc. Rev.* **2018**, *47*, 6744-6763.

(6) Auerbach, D. J.; Tully, J. C.; Wodtke, A. M. Chemical dynamics from the gas-phase to surfaces. *Nat. Sci.* **2021**, *1*, e10005.

(7) Nathanson, G. M. Molecular beam studies of gas-liquid interfaces. *Annu. Rev. Phys. Chem.* **2004**, *55*, 231-255.

(8) Tesa-Serrate, M. A.; Smoll, E. J., Jr.; Minton, T. K.; McKendrick, K. G. Atomic and molecular collisions at liquid surfaces. *Annu. Rev. Phys. Chem.* **2016**, *67*, 515-540.

(9) Nesbitt, D. J.; Zolot, A. M.; Roscioli, J. R.; Ryazanov, M. Nonequilibrium scattering/evaporation dynamics at the gas–liquid interface: wetted wheels, self-assembled monolayers, and liquid microjets. *Acc. Chem. Res.* **2023**, *56*, 700-711.

(10) Lednovich, S. L.; Fenn, J. B. Absolute evaporation rates for some polar and nonpolar liquids. *AIChE J.* **1977**, *23*, 454-459.

(11) Faubel, M.; Kisters, T. Non-equilibrium molecular evaporation of carboxylic acid dimers. *Nature* **1989**, *339*, 527.

(12) Lee, C.; Pohl, M. N.; Ramphal, I. A.; Yang, W.; Winter, B.; Abel, B.; Neumark, D. M. Evaporation and molecular beam scattering from a flat liquid jet. *J. Phys. Chem. A* **2022**, *126*, 3373-3383.

(13) Yang, W.; Lee, C.; Saric, S.; Pohl, M.; Neumark, D. Evaporation and scattering of neon, methane, and water from a dodecane flat liquid jet. *J. Chem. Phys.* **2023**, *159*, 054704.

(14) Saecker, M.; Govoni, S.; Kowalski, D.; King, M.; Nathanson, G. Molecular beam scattering from liquid surfaces. *Science* **1991**, *252*, 1421-1424.

(15) Saecker, M.; Nathanson, G. Collisions of protic and aprotic gases with hydrogen bonding and hydrocarbon liquids. *J. Chem. Phys.* **1993**, *99*, 7056.

(16) Lancaster, D. K.; Johnson, A. M.; Burden, D. K.; Wiens, J. P.; Nathanson, G. M. Inert Gas Scattering from Liquid Hydrocarbon Microjets. *J. Phys. Chem. Lett.* **2013**, *4*, 3045-3049.

(17) Fu, B.; Shan, X.; Zhang, D. H.; Clary, D. C. Recent advances in quantum scattering calculations on polyatomic

bimolecular reactions. *Chem. Soc. Rev.* **2017**, *46*, 7625-7649.
(18) Jiang, B.; Guo, H. Dynamics in reactions on metal surfaces: A theoretical perspective. *J. Chem. Phys.* **2019**, *150*, 180901.
(19) Li, J.; Zhao, B.; Xie, D.; Guo, H. Advances and new challenges to bimolecular reaction dynamics theory. *J. Phys. Chem. Lett.* **2020**, *11*, 8844-8860.
(20) Benjamin, I.; Wilson, M.; Pohorille, A. Scattering of Ne from the liquid–vapor interface of glycerol: A molecular dynamics study. *J. Chem. Phys.* **1994**, *100*, 6500-6507.
(21) Lipkin, N.; Gerber, R.; Moiseyev, N.; Nathanson, G. Atom scattering studies of liquid structure and dynamics: Collisions of Xe with a model of squalane. *J. Chem. Phys.* **1994**, *100*, 8408-8417.
(22) Peng, Y.; Liu, L.; Cao, Z.; Li, S.; Mazyar, O.; Hase, W.; Yan, T. Chemical dynamics simulation of ne atom scattering off a squalane surface. *J. Phys. Chem. C* **2008**, *112*, 20340.
(23) Wang, J.; Wolf, R. M.; Caldwell, J. W.; Kollman, P. A.; Case, D. A. Development and testing of a general AMBER force field (GAFF). *J. Comp. Chem.* **2004**, *25*, 1157.
(24) Alexander, W. A.; Zhang, J.; Murray, V. J.; Nathanson, G. M.; Minton, T. K. Kinematics and dynamics of atomic-beam scattering on liquid and self-assembled monolayer surfaces. *Faraday Discuss.* **2012**, *157*, 355-374.
(25) Mullins, C. B.; Rettner, C. T.; Auerbach, D. J.; Weinberg, W. H. Variation of the trapping probability of Ar on Pt(111) with kinetic energy and angle of incidence: The changing role of parallel momentum with surface temperature. *Chem. Phys. Lett.* **1989**, *163*, 111-115.
(26) Rettner, C.; Mullins, C.; Bethune, D.; Auerbach, D.; Schweizer, E.; Weinberg, W. Molecular beam studies of trapping dynamics. *J. Vac. Sci. Technol.* **1990**, *8*, 2699-2704.
(27) King, M. E.; Nathanson, G. M.; Hanning-Lee, M.; Minton, T. K. Probing the microscopic corrugation of liquid surfaces with gas-liquid collisions. *Phys. Rev. Lett.* **1993**, *70*, 1026-1029.
(28) King, M. E.; Fiehrer, K. M.; Nathanson, G. M.; Minton, T. K. Effects of thermal roughening on the angular distributions of trapping and scattering in gas–liquid collisions. *J. Phys. Chem. A* **1997**, *101*, 6556-6561.
(29) Perkins, B. G., Jr.; Nesbitt, D. J. Toward three-dimensional quantum state-resolved collision dynamics at the gas–liquid interface: theoretical investigation of incident angle. *J. Phys. Chem. A* **2009**, *113*, 4613-4625.

Figure 1. Slab model of the dodecane liquid surface and definitions of the coordinates and angles for in-plane scattering.

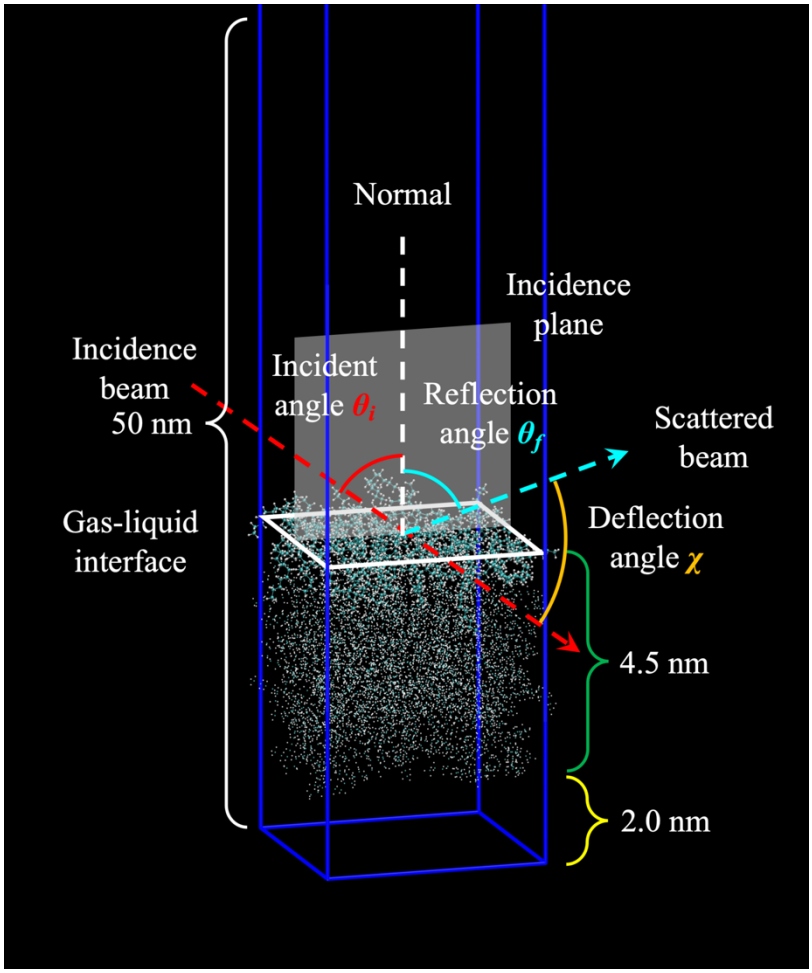

Figure 2. Exemplary trajectories. (a) is an IS trajectory, which encounters a single turning point (a kick) during the interaction with the surface. Trajectory (b) depicts a trapped Ne in the surface within the 500 ps simulation time. (c) is a typical TD trajectory, which experiences multiple turning points (kicks) and loses significant energy to the surface. In trajectory (d), the Ne travels across the surface like a skipping stone.

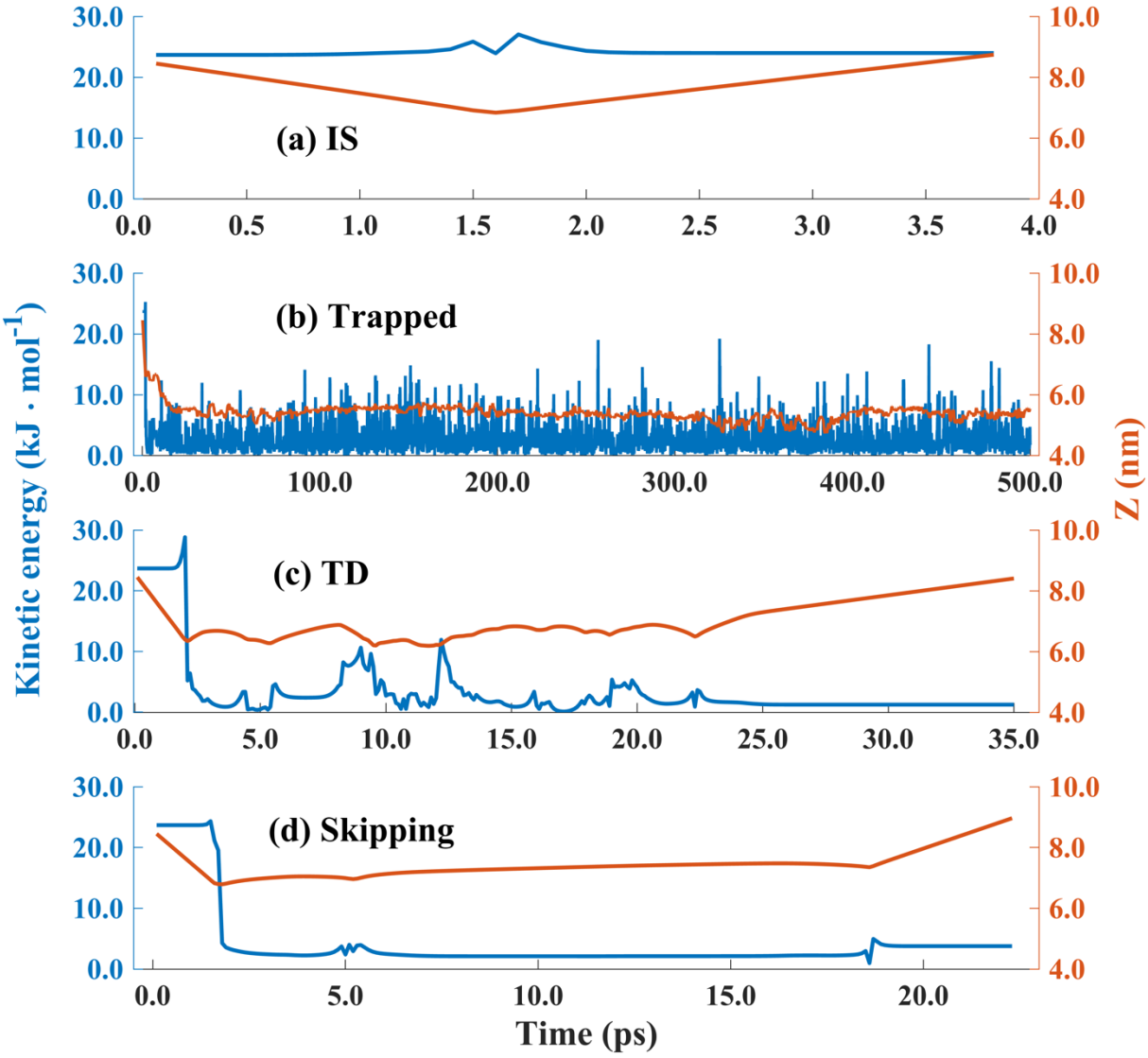

Figure 3. Calculated (MD) TD fractions at the reflection angle of $\theta_f = 60°$ as a function of incidence angle θ_i (a) and at an incidence angle $\theta_i = 60°$ as a function of the deflection angle χ (b) for fast (23.7 kJ/mol) and slow (6.3 kJ/mol) Ne. The experimental results[13] (Expt) are included for comparison.

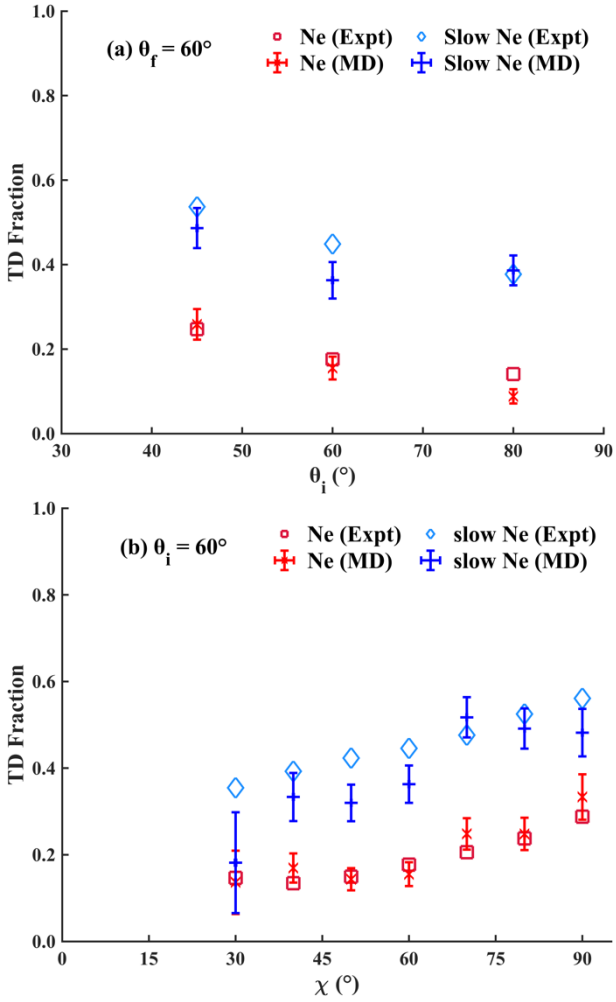

Figure 4. Normalized angular distributions of in-plane scattered Ne for several incidence energies and angles. The solid lines are $\cos\theta_f$ fits. The experimental distributions[13] are included for comparison.

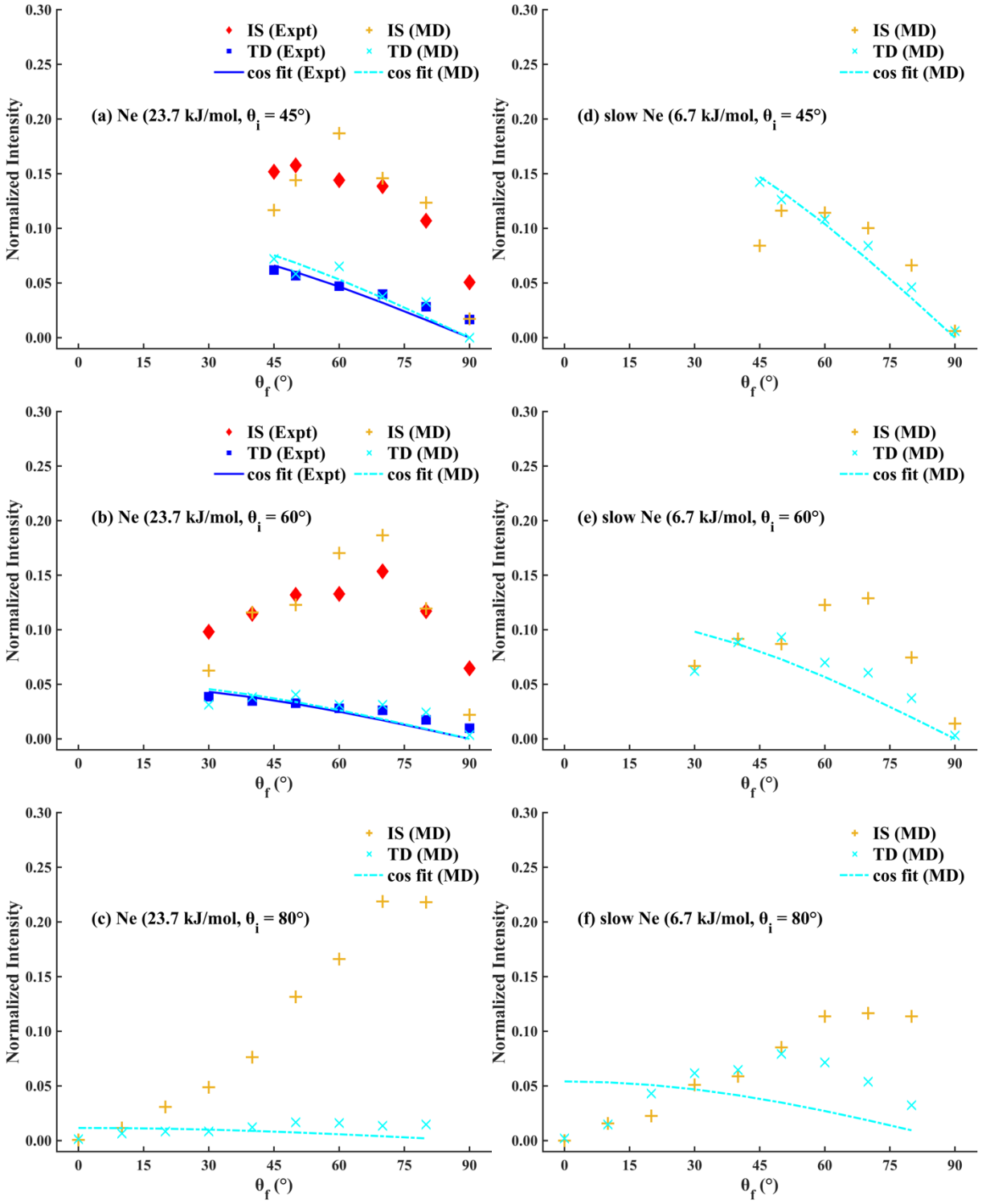

Figure 5. Calculated IS, TD, and total velocity distributions of the in-plane scattered Ne for several incidence energies and angles. The solid lines are fits according to Eqs. (1) and (2).

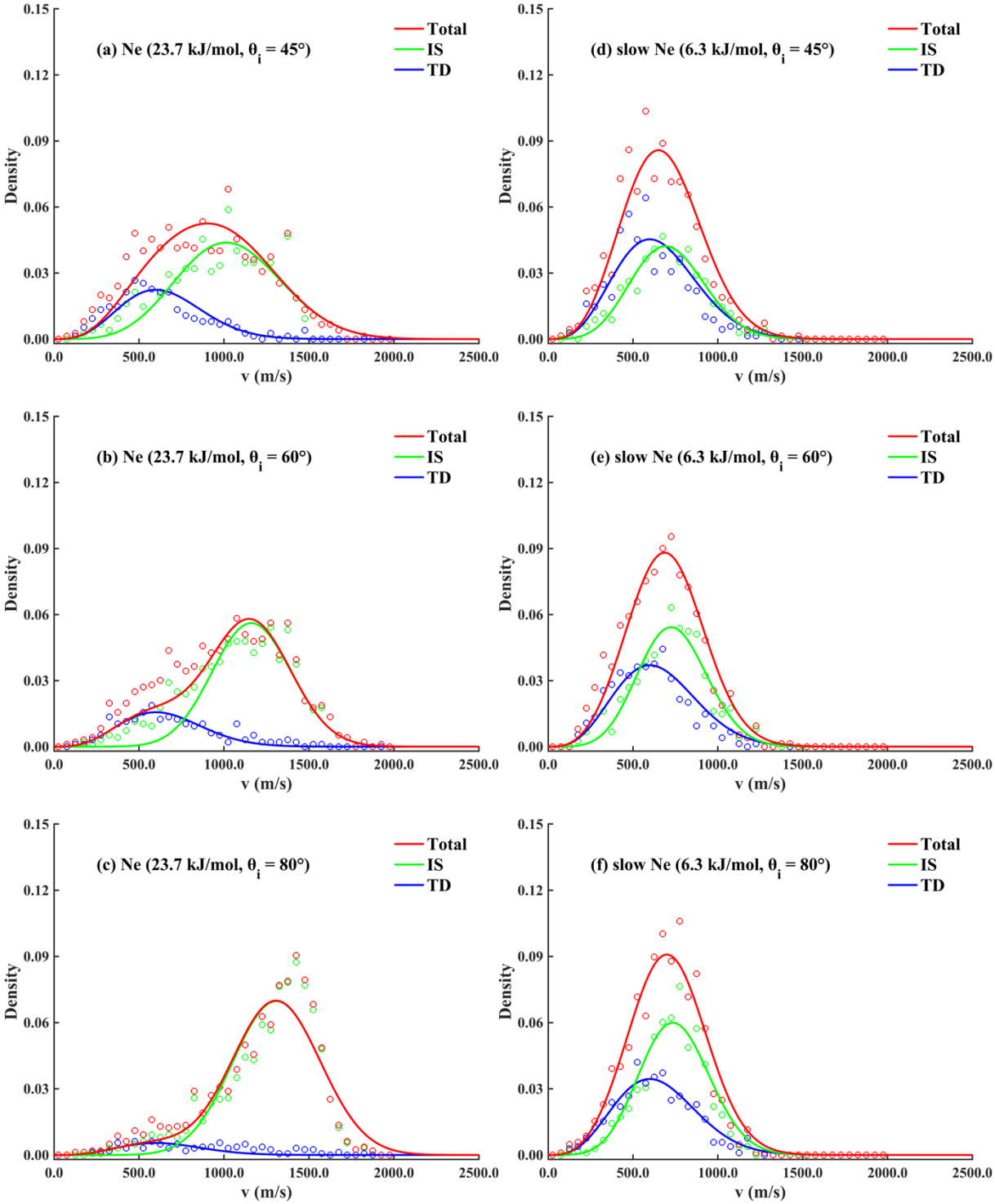

Figure 6. Calculated (MD) average fractional energy losses as a function of deflection angle χ for the IS channel of in-plane scattering of Ne at 23.7 kJ/mol. The experimental data[13] (Expt) are included for comparison.